Tunable Bragg peak response in liquid-crystal-infiltrated photonic crystals

Davy P. Gaillot, Elton Graugnard, Jeffrey S. King, and Christopher J. Summers

School of Materials Science and Engineering, Georgia Institute of Technology, Atlanta, Georgia, 30332-0245, USA

We report the dependence of the first-order Bragg peak position and width on the liquid-crystal and backbone refractive indices for liquid-crystal-infiltrated large-pore inverse shell opals, which offer increased volume for electro-optic infiltration. We also present the dependence of the photonic response on the template architecture or liquid-crystal volume fraction, which can be manipulated with a multilayer atomic layer deposition process. It is demonstrated from a three-dimensional finite-difference time-domain band structure and transmission–reflection coefficients computations that certain large-pore architectures exhibit an unusual optical response that cannot be explained by a classical Bragg peak theory. These structures potentially offer a pathway for all-optical photonic switching devices. © 2007 Optical Society of America

OCIS codes: 160.3710, 160.4330.

1. INTRODUCTION

Owing to their unique optical properties, photonic crystals hold the promise to overcome limitations in current optical devices with potential applications in waveguiding, beam steering, ultrafast switching, and demultiplexing.[1–3] Among three-dimensional (3D) photonic crystal structures, synthetic opals and inverse opals provide simple and effective approaches to creating, respectively, directional and complete photonic bandgaps (PBGs): frequency and spatial regions where no photons are allowed to propagate within the crystal.[4] A synthetic opal possesses a directional PBG along the densest close-packed $\Gamma - L$ direction, [111], and is experimentally characterized by a strong Bragg reflectance peak or transmission dip. The Bragg wavelength, λ_{Bragg}, is dependent on both the periodicity of the dielectric modulation and the effective refractive index, n_{eff}, of the material and at normal incidence is given by

$$\lambda_{\mathrm{Bragg}} = 2d_{111}n_{\mathrm{eff}} = 1.63Dn_{\mathrm{eff}} = \sqrt{2}D/\omega_{\mathrm{Bragg}}, \qquad (1)$$

where d_{111} is the spacing between (111) planes, D is the sphere diameter, and ω_{Bragg} is the normalized Bragg frequency. The effective refractive index, n_{eff}, of the opal structure can be controlled by the infiltration of a liquid crystal (LC) to tune λ_{Bragg}, as initially reported by Busch and John[5] and Yoshino *et al.*,[6] since LCs possess a birefringence, Δn_{LC}. When the orientation of the director is modified, the refractive index can be tuned between the ordinary (n_o) and the extraordinary (n_e) index values.[7] However, the low available volume fraction of an opal ($f_{\mathrm{LC}}^{\mathrm{opal}} = 0.26$) strongly limits director reorientation within the tetrahedral and octahedral interstitial sites,[8] resulting in reduced dielectric anisotropy. As a consequence, Bragg peak tuning with temperature or an applied electric field is severely limited.[6,8,9] On the other hand, inverse opals provide a larger void volume for LC infiltration and higher dielectric contrast, resulting in a wider

Bragg peak and complete PBGs, depending upon the backbone refractive index n_{BB}.[10] High-quality inverse shell opals can be fabricated by atomic layer deposition (ALD) of a high-index material onto the dielectric spheres to the maximum infiltration of 86% of the opal interstitial volume.[11–13] Removing the original dielectric template results in an inverse structure with a ~ 0.776 air volume fraction. This inverse opal can then be infiltrated with liquid crystal to a filling fraction of $f_{\mathrm{LC}} = 0.74$. In this configuration, the trapped tetrahedral and octahedral air pockets within the backbone contain the remaining air volume fraction, $f_{\mathrm{air}} = 0.036$. Since f_{LC} is increased from 0.26 in an infiltrated opal to 0.74 in an infiltrated inverse opal, it results in additional flexibility to tune n_{eff}, given by

$$n_{\mathrm{eff}} = (f_{\mathrm{BB}}n_{\mathrm{BB}}^2 + f_{\mathrm{LC}}n_{\mathrm{LC}}^2 + f_{\mathrm{air}}n_{\mathrm{air}}^2)^{1/2}, \qquad (2)$$

where f_{BB} is the backbone volume fraction of 0.224. Additionally, the volume fractions are related to one another by

$$f_{\mathrm{air}} + f_{\mathrm{LC}} + f_{\mathrm{BB}} = 1. \qquad (3)$$

However, the topology of conventional inverse shell opals hinders complete infiltration with LC molecules, owing to small interconnections (necking regions) between the spherical chambers. This can be experimentally overcome by sintering the template prior to infiltration, which results in the formation of large necks at the original sphere contact points and also increases the mechanical stability of the thin film.[10,13,14] Thus, inverting a sintered opal results in a low-filling-fraction backbone with spherical air chambers interconnected by large air pores.

Previously, we reported a multilayer ALD process based on the double conformal infiltration of a sacrificial material and high-index material to fabricate large-pore and non-close-packed inverse structures.[15] In this technique, a synthetic opal is first conformally infiltrated with a buffer material, followed by the conformal deposition of

a second layer to the maximum conformal infiltration volume of 22.4%. A large-pore inverse shell structure is formed after selective removal of the modified template (original opal and sacrificial shell). As a result of this process, as the sacrificial layer (SL) thickness is increased, the available volume fraction for LC infiltration increases, and the backbone volume fraction decreases. The SL ALD technique eliminates the need for sintering and provides a mechanism whereby f_{LC} and the effective refractive index, n_{eff}, can be finely adjusted by one's precisely controlling the backbone thickness. This also enables precise control of the pore size, which adds considerable geometrical flexibility and favors the reorientation of the LC molecules.

In this work, we report a study of the theoretical $\Gamma-L$ Bragg peak response on the average refractive index in LC-infiltrated large-pore inverse shell opals fabricated by the SL process. The Bragg peak shift of the tuned architectures was investigated by introducing a tuning ratio, $\Delta\lambda/\lambda_0$, interpreted as the shift of the Bragg peak wavelength, $\Delta\lambda$, with respect to the Bragg peak wavelength obtained at the lowest LC index, λ_0. The tuning ratio was derived from analytical equations. In contrast, photonic band diagrams were computed using the 3D finite-difference time-domain (FDTD) method (previously reported in a theoretical study of these structures)[15,16] to investigate the dependence of the Bragg peak position and width on the LC and backbone refractive indices and volume fractions, for structures fabricated using different template thicknesses (i.e., sacrificial shell radii). From these calculations, which were in good agreement with the classical theory, the positions of the pseudobandgaps are obtained by computation of the average Bragg frequency, ω_{Bragg}, of the second and third bands at the L point in the irreducible Brillouin zone. Additionally, the Bragg peak width, $\Delta\omega/\omega_{Bragg}$, given by the ratio of the difference in frequency between these bands to the average Bragg frequency, highlights the photonic crystal strength. Finally, the transmission–reflection coefficients of the investigated structures were simulated using the transfer-matrix method[17,18] with TRANSLIGHT using the $\langle 111 \rangle$ close-packed opal template.

2. ANALYTICAL ANALYSIS
The response of infiltrated LC to an applied electric field was modeled with an equivalent isotropic medium with average refractive index values, n_{LC}. The effective refractive index of the infiltrated structure can be expressed in terms of the investigated parameters: LC volume fraction, LC refractive index, and backbone refractive index. By substituting Eq. (3) in Eq. (2) and eliminating f_{BB}, Eq. (2) becomes

$$n_{eff} = n_{BB}[1 - f_{air}(1 - n_{air}^2/n_{BB}^2) - f_{LC}(1 - n_{LC}^2/n_{BB}^2)]^{1/2},$$
(4)

where the last term under the square root is negative whenever the refractive index of the backbone is greater than that of the LC and positive when smaller than the LC. When the two refractive indices are equal, the effective index is constant, and the structure behaves like a

quasi-isotropic optical medium, although air pockets remain trapped in the backbone. As a consequence, the Bragg peak is expected to collapse.

The tuning ratio, $\Delta\lambda/\lambda_0$, can then be analytically derived by combining the Bragg peak equation [Eq. (1)] for the lowest LC index, $\lambda_0(n_{LC}=1.5)=2d_{111}n_0$, and investigated LC index, $\lambda_1(n_{LC})=2d_{111}n_1$, where n_0 and n_1 are given by Eq. (2). The tuning ratio is given by

$$\Delta\lambda/\lambda_0 = (n_1 - n_0)/n_0 = n_1/n_0 - 1$$

$$= \left[\frac{1 + f_{LC}(n_{LC}^2/n_{BB}^2 - 1) + f_{air}(1/n_{BB}^2 - 1)}{1 + f_{LC}(1.5^2/n_{BB}^2 - 1) + f_{air}(1/n_{BB}^2 - 1)} \right]^{1/2} - 1.$$
(5)

Figure 1 presents the dependence of the tuning ratio for a range of structures and LC indices as predicted by Eq. (5). The LC refractive index was varied from 1.5 to 2.1, and the sacrificial shell radius R_{SL}, normalized to the sphere diameter D, was varied from 0.5115 to 0.5462. The inset schematic shows the fabrication parameters of the inverse scaffolds using the SL process. The structures present thick ($0.066D$) to thin ($0.0313D$) backbones. The corresponding LC filling-fraction values vary between 0.789 and 0.9045. To complete this study, low- to high-index backbone materials, which can typically be grown by ALD or chemical vapor deposition were employed: silica,[19] amorphous titania,[12] and silicon,[20] with refractive indices of 1.5, 2.31, and 3.45, respectively. The data clearly indicate that the dielectric contrast between the backbone material and the infiltrated LC plays a major role in enhancing the tuning range of the structure, which can approach 40% of λ_0 ($n_{LC}=1.5$). Of the three types of backbone, the maximum shift of $\sim$37% is obtained for the structure with the lowest index (silica). Furthermore, as
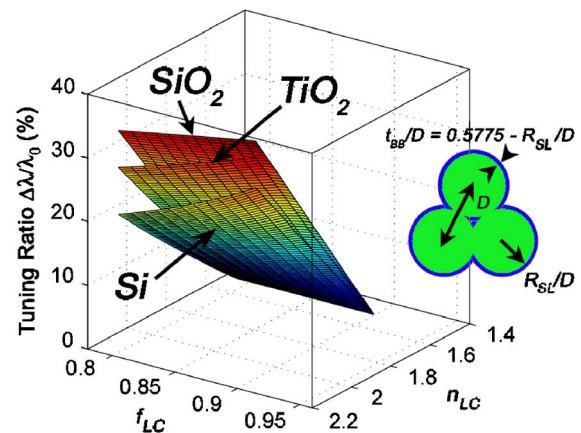

Fig. 1. (Color online) Dependence of theoretical tuning ratio on the fabrication parameters obtained from Eq. (5). The LC refractive index was varied from 1.5 to 2.1 and the sacrificial shell radius R_{SI}/D was varied from 0.5115 to 0.5462 (corresponding to LC filling-fraction values between 0.789 and 0.9045). Three backbone materials were used: silica, amorphous titania, and silicon, with refractive indices of 1.5, 2.31, and 3.45, respectively. The inset shows the structural parameters of an infiltrated opal fabricated by a SL process and used in the 3D FDTD simulations.
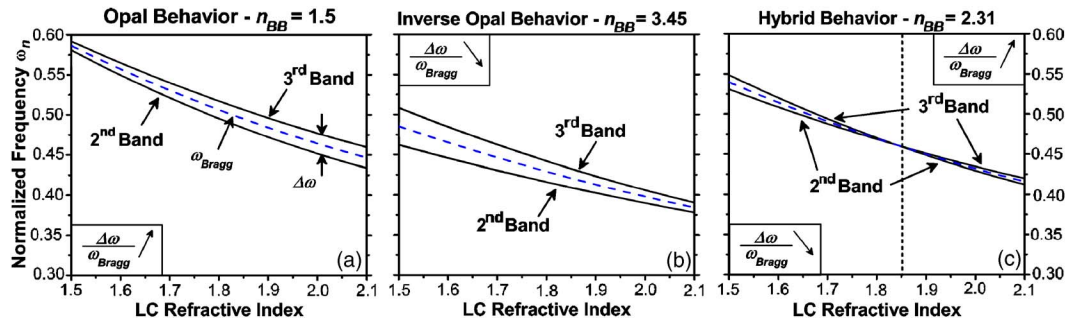
Fig. 2.   (Color online) Dependence of the $\Gamma-L$ Bragg peak response on the LC index in a tuned large-pore inverse opal fabricated with a backbone thickness of 0.066D. For all cases, the lower and upper curves represent the second and third bands defining the first-order $\Gamma-L$ photonic gap, respectively. The dotted curve shows the locus of the Bragg peak frequency, ω_{Bragg}. (a) The backbone material is silica ($n_{\text{LC}}=1.5$), and the structure exhibits an opallike behavior. (b) The backbone material is silicon or GaP ($n_{\text{LC}}=3.45$), and the structure exhibits an inverse opallike behavior. (c) The backbone material is amorphous titania ($n_{\text{LC}}=2.31$); consequently, the structure exhibits an inverse opallike behavior for LC index values below 1.85 and an opallike behavior for values above 1.85.

the backbone index is increased (i.e., the dielectric contrast is increased), the tuning ratio decreases ($\sim35\%$ for titania and $\sim30\%$ for silicon). For the best-case scenario for maximum Bragg peak shift (silica backbone), the tuning ratio exhibits a small dependence on the LC volume fraction. In contrast, for larger backbone index values (silicon), the tuning ratio shows a strong dependence on the LC volume fraction. On the basis of this preliminary study, we conclude that maximum tuning is obtained with the lowest dielectric contrast, regardless of the LC filling fraction.

3. FINITE-DIFFERENCE TIME-DOMAIN SIMULATIONS

A. Backbone Index Dependence on the Optical Response
Unfortunately, the photonic crystal strength (i.e., Bragg peak width) can neither be extrapolated from this analysis nor derived from analytical equations. As a consequence, computational tools such as FDTD must be used to predict the PBG properties of the structures discussed above. From the simulated photonic band structures, the dependence of the normalized Bragg peak frequency, ω_{Bragg}, and the stop-band edges (i.e., second and third bands along the L direction) on the LC index can be extracted. The Bragg peak position and width directly define the optical response of the tuned structure. Thus, the tuning ratio and Bragg peak width, $\Delta\omega/\omega_{\text{Bragg}}$, can be easily extracted from the FDTD data. As an example of this approach, the photonic band structures of LC-infiltrated inverse structures presenting a thick backbone t_{BB}/D of 0.066 ($R_{\text{SL}}/D=0.5115$) were investigated as a function of the LC index. Figures 2(a)–2(c) present the summary of these simulations for silica, amorphous titania, and silicon backbone materials, respectively. This set of data indicates that the optical response of the tuned structure is strongly dependent on the backbone index or dielectric contrast and results in three types of behavior.

In the first scenario investigated, the LC index is equal to or greater than the backbone index (silica). Analysis of Fig. 2(a) shows that, as the LC index is increased, the frequency of the second band (dielectric band) shifts at a faster rate than the third (air band). Since the dielectric

contrast is increased, it follows that the Bragg peak width increases. This behavior is typically observed in bare opals where increasing the sphere index contributes to enlarging the $\Gamma-L$ stop band. This is usually attributed to the electromagnetic fields being concentrated within the highest dielectric regions of the structure: the LC network that mimics that of an opal.

For high-index backbone structures (silicon), the opposite behavior is predicted. Figure 2(b) shows that the Bragg peak width decreases with LC index because the frequency of the upper band now shifts down at a faster rate than the lower band. This behavior is typically encountered in inverse shell opals where decreasing the dielectric contrast negatively affects (reduces) the width of the stop band. Indeed, the electromagnetic fields concentrated within the highest dielectric regions of the structure (dielectric skeleton) will be redistributed toward the LC material when its index is increased.

From this analysis, one can immediately conclude that structures exhibiting both behaviors must exist to preserve band-to-band continuity. In fact, Fig. 2(c) presents the results for the intermediate backbone index (amorphous titania). This figure clearly demonstrates that the tuned photonic crystal exhibits an unusual hybrid behavior. As the LC index is increased from 1.5, the Bragg peak width is reduced and eventually completely collapses for a LC index of 1.85. At this threshold value, the lower and upper bands touch each other ($\Delta\omega=0$), and the structure abruptly becomes highly transparent. In this region, the dielectric topology is such that the structure optically behaves like an inverse opal, as mentioned previously for a silicon backbone. For LC index values above the threshold value, the stop band is recovered and widens for further increases in the LC index. One may expect that the dielectric topology would behave like an inverse shell opal, since the backbone index is greater than the LC index, and therefore the electromagnetic fields would be concentrated in the backbone. In contrast, the data show that the fields diffuse toward the LC material, although the dielectric contrast is above 1.1 for all cases. This phenomenon has been reported by García-Santamaría *et al.* for an opal step infiltrated with Ge.[21] However, no structures have been reported in which it is possible to dynamically tune through the collapse of the Bragg peak. This opens

the door for a unique class of photonic devices whose optical stop band can be dynamically switched on and off (reflect–transmit light) with an applied electric field, provided that the LC has a sufficiently large dielectric anisotropy at the on–off threshold value.

B. Backbone Thickness Study

In this subsection, the dependence of the PBG properties on the backbone thickness in tuned large-pore structures was investigated. Additionally, the data for the thickest backbones ($0.066D$) were computed from the data presented in Fig. 2.

First, the PBG properties of inverse structures with the lowest backbone index were investigated. Figures 3(a) and 3(b) show the dependence of the Bragg peak width and tuning ratio, respectively, obtained from FDTD simulations to the LC index in a silica inverse opal ($n_{BB}=1.5$), fabricated with various sacrificial shell radii. Again, the average LC refractive index was varied from 1.5 to 2.1 for sacrificial shell radii R_{SL}/D of 0.5115, 0.5234, 0.5346, and 0.5462 (corresponding to LC filling-fraction values of 0.789, 0.8341, 0.8715, and 0.9045, respectively) as in Section 2.

As discussed previously, this type of structure mimics an opal with a dielectric contrast that increases with LC refractive index, and the Bragg peak width was predicted to increase. For all backbone thicknesses, the data show that the Bragg peak width monotonically increases with LC index to a maximum value as the LC reaches its highest refractive index of 2.1. However, the formation of thinner backbones negatively affects the Bragg peak width whereas the tuning ratio is slightly enhanced, as the LC refractive index is increased. The resulting predicted tuning ratio slope is ~50% (when the LC index is tuned by ±0.1, the Bragg peak accordingly shifts by ±5%). Since thinner backbones favor a larger LC volume fraction, the infiltrated material plays a more predominant role in tuning the Bragg peak position. However, owing to the low dielectric properties of the backbone, the structure closely resembles a homogenous medium and rapidly loses its

Fig. 4.   (Color online) Transmission spectra of tuned-silica large-pore inverse opals ($n_{BB}=1.5$) with a backbone thickness of $0.066D$, for LC refractive index values between 1.5 and 2.1. The spectra have been vertically translated for clarity. The transmission coefficients were simulated using the TRANSLIGHT package.

Fig. 5.   (Color online) (Color online) Bragg peak response of tuned-TiO$_2$ large-pore inverse opals ($n_{BB}=2.31$) for backbone thicknesses between $0.066D$ and $0.0313D$. (a) Dependence of the Bragg peak width on the LC refractive index. (b) Dependence of the relative tuning ratio. The dashed curves in (a) and (b) show a comparison between experimental data after Graugnard and coworkers[14] and theoretical data presented in this paper.

PBG properties. It is noteworthy that the tuning ratio predicted by the FDTD computation agrees well with the data presented in Fig. 1 and obtained by Eq. (5).

Additionally, the dependence of the transmission spectrum on the LC index of the structure with the thickest backbone (thinnest SL of $0.5115D$) was simulated. This data, shown in Fig. 4, confirm that a narrow notch in the transmission is present for the lowest LC index, resulting in a sharp Bragg peak as expected. For LC index values increasing from 1.5 to 2.1, the transmission notch is observed to shift down in frequency owing to the effective increase in refractive index. Thus, the notch width is increased, indicating that a broader Bragg peak is supported. These data are in good agreement with the FDTD simulations presented in Fig. 3(a).

In a second configuration, the backbone material has a refractive index slightly larger than the maximum LC refractive index. This type of structure was found to exhibit the anomalous hybrid behavior whereby the Bragg peak width was predicted to decrease, disappear, and increase. Figures 5(a) and 5(b) show the Bragg peak width and tun-
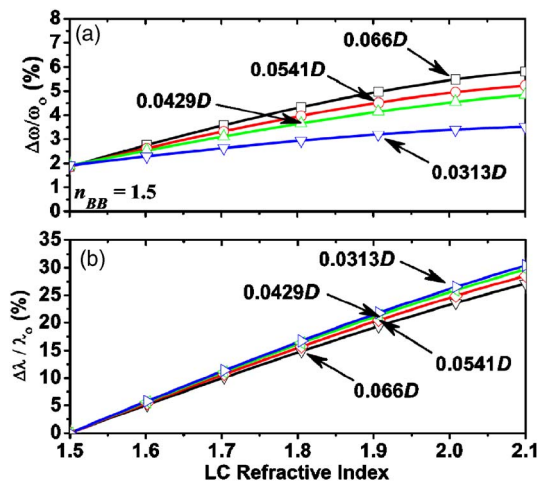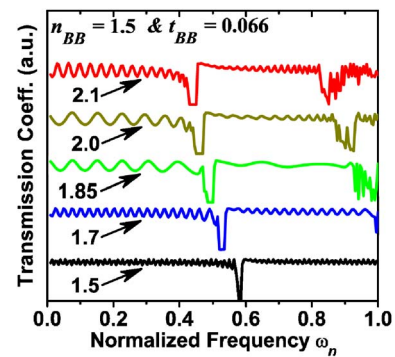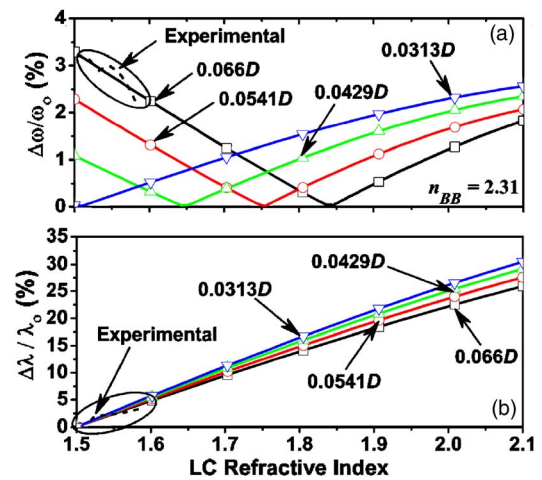

Fig. 3.   (Color online) Bragg peak response of tuned-silica large-pore inverse opals ($n_{BB}=1.5$) for backbone thicknesses between $0.066D$ and $0.0313D$. (a) Dependence of the Bragg peak width on the LC refractive index. (b) Dependence of the relative tuning ratio (fraction of Bragg peak normalized frequency at $n_{LC}=1.5$).

ing ratio, respectively, as a function of the infiltrated LC index in an amorphous TiO_2 inverse opal (n_{BB}=2.31). Again, the backbone thickness was varied from 0.066D (thickest backbone) to 0.0313D (thinnest backbone), and the LC index values were varied from 1.5 to 2.1.

The data presented in Fig. 5(a) indicate that the formation of thinner backbone structures (achieved by the use of thick SL) strongly affects the optical response of the tuned structure. Although the two inverse opal–opal behaviors still coexist, a thinner backbone promotes a broader Bragg peak width in the second opal region, whereas it continuously attenuates the Bragg peak width in the first inverse opal region. For ultrathin backbone templates, the first region is even predicted to disappear, and the structure now behaves like an opal. Moreover, the threshold value at which the Bragg peak width collapses shifts toward lower LC index values. This result is quite important as it enables the use of LC molecules with lower refractive indices to optically switch the Bragg peak on and off. One can now simply engineer the host template with ALD so that the threshold value occurs within the LC index range. Figure 5(b) shows that the tuning ratio exhibits the same dependence on the backbone thickness as for the silica backbone.

Recently, Graugnard and co-workers fabricated a LC-infiltrated TiO_2 large-pore inverse opal and reported a 20 nm Bragg peak shift by tuning the 5CB LC refractive index from n_e=1.583 to n_o=1.522 with an applied electric field of 50 V.[14] Their large-pore structure was synthesized using a mild sintering process and was roughly equivalent to a structure fabricated with a sacrificial shell radius value R_{SL}/D of ~0.5115 (backbone thickness t_{BB}/D of 0.066). Their experimental data, presented in Figs. 5(a) and 5(b), are in excellent agreement with the FDTD results and support the feasibility of fabricating tuned structures with an on–off Bragg peak switch.

The dependence of the transmission spectrum on the LC index for structures with a backbone thickness of 0.066 is presented in Fig. 6. The data clearly indicate that as the LC is increased from 1.5 to 1.85 the Bragg peak width decreases. At the threshold value (1.85), the medium no longer supports the Bragg peak and optically behaves like a homogeneous medium, thus confirming the
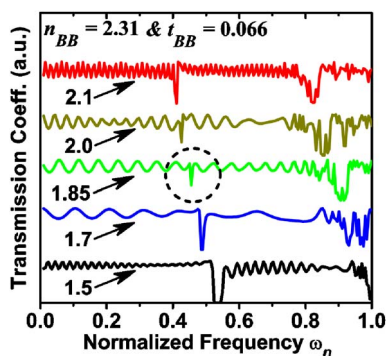

Fig. 7.   (Color online) Bragg peak response of tuned-silicon or gallium phosphide large-pore inverse opals (n_{BB}=3.45) for backbone thicknesses between 0.066D and 0.0313D. (a) Dependence of the Bragg peak width on the LC refractive index. (b) Dependence of the relative tuning ratio. For a backbone thickness $t_{BB}/D < 0.0429$, the structure becomes transparent for a range of LC index values, as indicated, for example, with $t_{BB}/D = 0.0313$ and LC index values ranging between ~1.9 and 2.1.

FDTD data. On the other hand, as the LC index is increased now from 1.85 to 2.1, the Bragg peak recovers and increases in width.

In the final configuration considered, the backbone material has the largest refractive index discussed in this work. This type of structure exhibits an inverse opal behavior, and the Bragg peak width is predicted to decrease with the LC index. Figures 7(a) and 7(b) show the dependence of the Bragg peak width and tuning ratio, respectively, on tuning the LC in an infiltrated silicon or gallium phosphide inverse opal (n_{BB}=3.45). As before, the backbone thickness was varied from 0.066D (thickest backbone) to 0.0313D (thinnest backbone). The tuning ratio data, presented in Fig. 7(b), remain close to the previous data [Figs. 1, 3(b), and 5(b)]. It is noteworthy that the slope of the tuning ratio is lower. This is also attributed to the large dielectric contrast between the backbone and the infiltrated materials. The data in Fig. 7(a) indicate that the Bragg peak widths for n_{LC}=1.5 and 2.1 are larger compared with the previous cases (n_{BB}=1.5 and 2.31). However, when the backbone thickness is decreased, the Bragg peak width at both minimum and maximum LC refractive values decreases. Again, this is attributed to the decreasing influence of the dielectric backbone. It follows that the Bragg peak eventually collapses. However, the Bragg peak does not reappear as previously observed with further increase of the LC index, and only the inverse opallike behavior (first case considered) is encountered. For a backbone thickness of 0.0313D, the LC index threshold is ~1.9. The second optical behavior (opallike) would be expected to appear for much greater LC index values, since the backbone index is so much larger. As a consequence, the material behaves like a transparent medium for a wide range of LC index values. These structures mimic electrical diodes whereby a certain LC index threshold (voltage) is required to increase the Bragg peak width (current), with potential applications in all-optical circuitry.

Fig. 6.   (Color online) Transmission spectra of tuned-TiO_2 large-pore inverse opals (n_{BB}=2.31) with a backbone thickness of 0.066D, for LC refractive index values between 1.5 and 2.1. The spectra have been vertically translated for clarity. The dashed circle indicates structures for which the Bragg peak has collapsed.
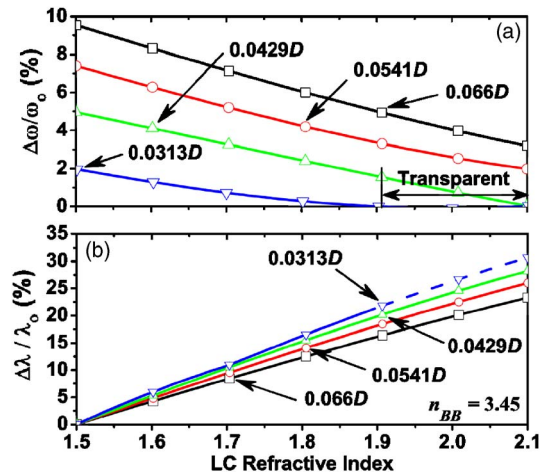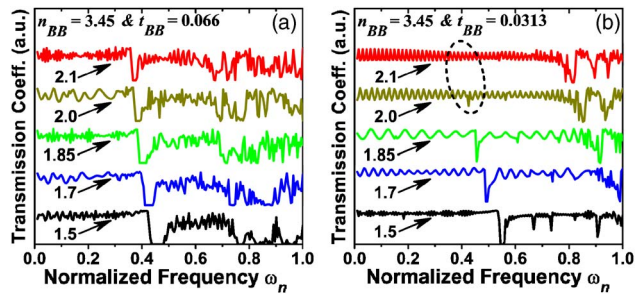
Fig. 8. (Color online) Transmission spectra of tuned-silicon or gallium phosphide large-pore inverse opals ($n_{BB}=3.45$) for LC refractive index values between 1.5 and 2.1. The spectra have been vertically translated for clarity. (a) Large-pore structure with a backbone thickness of $0.066D$. (b) Large-pore structure with a backbone thickness of $0.0313D$. The dashed circle indicates structures for which the Bragg peak has collapsed.

Finally, the transmission spectrum dependence on the LC index for the structures with the thickest (t_{BB}/D $=0.066$) and thinnest backbones ($t_{BB}/D=0.0313$) were simulated. The data are presented in Figs. 8(a) and 8(b), respectively. Figure 8(a) clearly indicates that as the LC is increased from 1.5 to 2.1 the transmission notch width or Bragg peak width decreases, and the structure slowly loses its PBG effect. However, Fig. 8(b) shows that the Bragg peak slowly disappears for LC index values increasing from 1.5 to 1.9, thus strongly supporting the FDTD results. Further increase of the LC index reinforces this phenomenon, and no Bragg peak is predicted for LC index values greater than 2.0, at which point the material becomes highly transparent.

4. CONCLUSION

In conclusion, we report the theoretical response of the first-order $\Gamma-L$ Bragg peak in LC-infiltrated large-pore inverse opals fabricated with a wide range of materials and backbone thicknesses. The results demonstrate that the Bragg peak tunability (width and location) is strongly dependent on the dynamic LC director reorientation and dielectric contrast between the backbone and the LC material. A ~50% average tuning ratio slope was predicted for all large-pore inverse structures investigated that offer reduced volume for electro-optical material infiltration. Most importantly, a strong dependence of the Bragg peak response on the backbone material and geometry was demonstrated through the simulation of transmission coefficients and photonic band structures. Three optical behaviors were predicted and discussed. Tuned structures with low-index backbones ($n_{BB}<n_{LC}$) exhibit an opallike behavior, whereas structures with high-index backbones ($n_{BB}=3.45$) exhibit an inverse opallike behavior. Surprisingly, tuned structures with intermediate-index backbones ($n_{BB}=2.31$) were found to exhibit both behaviors; the transition threshold was dependent on the backbone thickness (LC volume fraction). As a consequence, the Bragg peak tuning range is decreased, increased, and partially or totally canceled in structures with backbone indices larger than the maximum LC index. Moreover, it was found that static adjustments of the large-pore scaffold that can be implemented by using a SL ALD process allow the threshold index value at which the

Bragg peak switching phenomenon occurs to be finely adjusted. Therefore, LC-infiltrated large-pore inverse opals fabricated with a SL ALD technique provide a robust pathway to design photonic devices with unique transmission–reflection properties. This potentially enables all-optical switching devices with commercial electro-optical materials such as LC.

ACKNOWLEDGMENTS

REFERENCES

1. S. John, "Strong localization of photons in certain disordered dielectric superlattices," Phys. Rev. Lett. **58**, 2486–2489 (1987).
2. E. Yablonovitch, "Inhibited spontaneous emission in solid-state physics and electronics," Phys. Rev. Lett. **58**, 2059–2062 (1987).
3. R. Zengerle, "Light propagation in singly and doubly periodic planar waveguides," J. Mod. Opt. **34**, 1589–1617 (1987).
4. W. L. Vos, M. Megens, C. M. van Kats, and P. Bosecke, "Transmission and diffraction by photonic colloidal crystals," J. Phys. Condens. Matter **8**, 9503–9507 (1996).
5. K. Busch and S. John, "Liquid-crystal photonic-band-gap materials: the tunable electromagnetic vacuum," Phys. Rev. Lett. **83**, 967–970 (1999).
6. K. Yoshino, Y. Shimoda, Y. Kawagishi, K. Nakayama, and M. Ozaki, "Temperature tuning of the stop band in transmission spectra of liquid-crystal infiltrated synthetic opal as tunable photonic crystal," Appl. Phys. Lett. **75**, 932–934 (1999).
7. I.-C. Khoo, *Liquid Crystals: Physical Properties and Nonlinear Optical Phenomena* (Wiley, 1995).
8. D. Kang, J. E. Maclennan, N. A. Clark, A. A. Zakhidov, and R. H. Baughman, "Electro-optic behavior of liquid-crystal-filled silica opal photonic crystals: effect of liquid-crystal alignment," Phys. Rev. Lett. **86**, 4052–4055 (2001).
9. Y. Shimoda, M. Ozaki, and K. Yoshino, "Electric field tuning of a stop band in a reflection spectrum of synthetic opal infiltrated with nematic liquid crystal," Appl. Phys. Lett. **79**, 3627–3629 (2001).
10. K. Busch and S. John, "Photonic band gap formation in certain self-organizing systems," Phys. Rev. E **58**, 3896–3908 (1998).
11. A. Rugge, J. S. Becker, R. G. Gordon, and S. H. Tolbert, "Tungsten nitride inverse opals by atomic layer deposition," Int. Chem. Eng. **3**, 1293–1297 (2003).
12. J. S. King, E. Graugnard, and C. J. Summers, "TiO_2 inverse opals fabricated using low-temperature atomic layer deposition," Adv. Mater. (Weinheim, Ger.) **17**, 1010–1013 (2005).
13. J. S. King, D. P. Gaillot, E. Graugnard, and C. J. Summers, "Conformally back-filled, non-close-packed inverse-opal photonic crystals," Adv. Mater. (Weinheim, Ger.) **18**, 1063–1067 (2006).
14. E. Graugnard, J. S. King, S. Jain, and C. J. Summers, "Electric-field tuning of the Bragg peak in large-pore TiO_2 inverse shell opals," Phys. Rev. B **72**, R233105 (2005).
15. E. Graugnard, J. S. King, D. P. Gaillot, and C. J. Summers, "Sacrificial-layer atomic layer deposition for fabrication of non-close-packed inverse-opal photonic crystals," Adv. Funct. Mater. **16**, 1187–1196 (2006).
16. D. P. Gaillot and C. J. Summers, "Photonic band gaps in

non-close-packed inverse opals," J. Appl. Phys. **100**, 113118–113128 (2006).

17. P. M. Bell, J. B. Pendry, L. Martin Moreno, and A. J. Ward, "A program for calculating photonic band structures and transmission coefficients of complex structures," Comput. Phys. Commun. **85**, 306–322 (1995).

18. J. B. Pendry and A. MacKinnon, "Calculation of photon dispersion relations," Phys. Rev. Lett. **69**, 2772–2775 (1992).

19. H. Miguez, N. Tetreault, S. M. Yang, V. Kitaev, and G. A. Ozin, "A new synthetic approach to silicon colloidal photonic crystals with a novel topology and an omnidirectional photonic bandgap: micromolding in inverse silica opal (MISO)," Adv. Mater. (Weinheim, Ger.) **15**, 597–600 (2003).

20. A. Blanco, E. Chomski, S. Grabtchak, M. Ibisate, S. John, S. W. Leonard, C. Lopez, F. Meseguer, H. Miguez, J. P. Mondla, G. A. Ozin, O. Toader, and H. M. van Driel, "Large-scale synthesis of a silicon photonic crystal with a complete three-dimensional bandgap near 1.5 micrometers," Nature **405**, 437–440 (2000).

21. F. Garcia-Santamaria, M. Ibisate, I. Rodriguez, F. Meseguer, and C. Lopez, "Photonic band engineering in opals by growth of Si/Ge multilayer shells," Adv. Mater. (Weinheim, Ger.) **15**, 788–792 (2003).